

1 **Deriving probabilistic soil distribution coefficients (K_d). Part 1: General**
2 **approach to decreasing and describing variability and example using**
3 **uranium K_d values**

4 Oriol Ramírez-Guinart^a, Daniel Kaplan^b, Anna Rigol^{*,a}, and Miquel Vidal^a

5 ^a *Chemical Engineering and Analytical Chemistry Department, Faculty of Chemistry,*
6 *University of Barcelona, Martí i Franqués 1-11, 08028, Barcelona, Spain.*

7 ^b *Savannah River National Laboratory, Aiken, South Carolina, USA*

8

9 *Corresponding author: Telephone: (+34) 93 403 9274; Fax: (+34) 93 402 1233

10 *Email address: annarigol@ub.edu (A. Rigol)*

11

12

13

14

15

16

17 **Acknowledgements**

18 This work was carried out in the frame of the IAEA MODARIA and MODARIA II
19 programmes. It was supported by the Ministerio de Ciencia e Innovación de España
20 (CTM2014-55191 and CTM2017-87107-R), the Generalitat de Catalunya (2017 SGR 907),
21 the Argonne Wetland Hydrobiogeochemistry Scientific Focus Area funded by the Department
22 of Energy's Office of Sciences, Subsurface Biogeochemistry Research Program (DE-AD09-
23 96SR18500), and the Savannah River National Laboratory's LDRD program (LDRD-2017-
24 00005). Oriol Ramírez would like to thank the support of an APIF pre-doctoral fellowship
25 from the University of Barcelona. Authors would also like to thank Dr. Brenda Howard for
26 her fruitful discussions and Oriol Toll for his contribution in data treatment.

1 Deriving probabilistic soil distribution coefficients (K_d). Part 1: General 2 approach to decreasing and describing variability and example using 3 uranium K_d values

4

5 **Abstract**

6 A general approach is presented to derive probabilistic radionuclide distribution coefficients
7 (K_d) in soils from a K_d dataset. The main aim was to derive informed estimates with a low
8 inherent uncertainty by restricting the K_d value data to subsets based on key soil factors and
9 the experimental approach used to calculate the K_d value (e.g., sorption and desorption tests).
10 As an example, the general approach was applied to uranium (U) K_d values that are part of a
11 critically reviewed dataset containing more than 5000 soil K_d entries for 83 elements and an
12 additional 2000 entries of K_d data for 75 elements gathered from a selection of other, non-soil,
13 geological materials. The overall soil U K_d dataset included 196 values spanning a range of
14 four orders of magnitude (1 to 67,000 L kg⁻¹), with additional 50 entries for other geological
15 materials. Whereas the effect of the experimental approach could be disregarded, major
16 factors in decreasing U K_d variability were pH and organic matter concentration (OM).
17 Limitation in the number of entries made it difficult to use texture information (sand, silt,
18 clay) to further decrease U K_d variability. The integrated combination of pH+OM permitted
19 some soil groups to have U K_d confidence intervals as narrow as two orders of magnitude.
20 Specifically for U K_d , data in the Mineral (<20% OM) and Organic (\geq 20% OM) partial
21 datasets were significantly different. Analogue data from geological materials other than soils,
22 such as subsoil, till and gytja (a lacustrine mud containing elevated organic matter (OM)
23 concentrations), were also statistically evaluated to determine whether they could be used to
24 fill U K_d data gaps. It was shown that U K_d from subsoils and tills, but not gytjas, could be
25 used to enhance soil U K_d datasets. Selection of probabilistic K_d values for risk modelling can
26 be made more reliably and with less uncertainty by using appropriate geochemical data
27 representative of the study site to narrow the wide range of potential K_d values.

28

29 **Keywords**

30 Distribution coefficient; radionuclide; soil; cumulative distribution function; uranium;
31 probabilistic modeling

32 **1. Introduction**

33 The partitioning of radionuclides (RN) between solid and liquid phases largely affects the RN
34 mobility and bioavailability in soils. RN partitioning is often quantified by the solid-liquid
35 distribution coefficient (K_d), defined as the ratio of activity concentration of RN sorbed on a
36 specified solid phase (C_{solid}) to the RN activity concentration in a specified liquid phase
37 (C_{liquid}) in equilibrium with the former (ICRU, 2001). Despite that the K_d model is based on
38 several theoretical assumptions, which are not always fulfilled (EPA, 1999a), its use
39 constitutes the simplest sorption model available. Risk assessment models use soil K_d values
40 to derive RN concentration in solution from the concentrations of RNs in contaminated soils
41 to estimate: the transfer of the bioavailable pool of RNs between soil layers and to plants, the
42 leaching of RNs from the surface of contaminated soils and further transport in the
43 unsaturated zone (vadose zone) and saturated zone (groundwater), and the diffusion-driven
44 transport of RN through soils (Simon-Cornu et al., 2015; Sy et al., 2016).

45 The K_d parameter alone does not give information about the sorption mechanisms
46 governing the phase partitioning of the target species. Reported K_d values of RNs can vary
47 greatly due to the experimental methods used for their quantification. Among the methods
48 used to measure K_d values are: 1) in situ measurements of RN concentrations in paired
49 samples of soil and porewater collected from the field; 2) batch uptake tests with dispersed
50 samples and RN-spiked aqueous phase; 3) desorption tests with RN-contaminated soils; and
51 4) dynamic column flow experiments or dynamic tank-leaching tests with compacted samples
52 (OECD, 2000; ASTM, 2003; Gil-García et al., 2008; ASTM, 2010; Aldaba et al., 2010; EPA,
53 2017). To complicate matters further, several experimental parameters also influence the
54 measured K_d values, including contact time of the RN and soil, the soil:solution ratio, and
55 solution chemical characteristics that is in contact with the soil during the uptake or
56 desorption experiments.

57 To make the K_d data derived from compilations suitable for risk assessment purposes,
58 it must be ensured that they were derived from experiments using similar solids, liquids, and
59 RN species as exist at the contamination scenario under study. This requires identifying the
60 factors controlling the RN-soil interaction to explain, and when possible to reduce, the K_d
61 variability. Ideally, risk assessments models use site-specific K_d values, however such data are
62 often not available. To overcome this limitation, probabilistic models are a useful option
63 (Degryse et al., 2009). Probabilistic models use K_d compilations to derive, among other
64 parameters, the most likely/best-estimate K_d values, statistical functions describing the overall
65 variability of K_d values, and to derive confidence intervals at specified significance levels

66 (Sheppard and Thibault, 1990; Stenhouse, 1994; EPA, 2001; Simon-Cornu et al., 2015).
67 However, the derived statistics from these K_d compilations are often suitable only for
68 screening purposes because the variability is high. One approach to reducing this variability is
69 to create K_d data subsets for different soil types based on the soil characteristics governing the
70 target RN sorption in soils, if this information is available (IAEA, 2010) and describing K_d
71 variability by using distribution functions, so the input data in risk assessment models are
72 entered with their variability thus contributing to the final uncertainty derived from the
73 application of the model.

74 The International Atomic Energy Agency (IAEA) launched the Environmental
75 Modelling for Radiation Safety Programme (EMRAS) (2003-2007), whose main purpose was
76 to identify and reduce uncertainties in the predictive capability of environmental models. The
77 EMRAS Programme produced the Technical Report Series 472 'Handbook of Parameter
78 Values for the Prediction of Radionuclide Transfer in Terrestrial and Freshwater
79 Environments' (IAEA, 2010), and a related TECDOC 1616 document entitled, 'Quantification
80 of radionuclide transfer in terrestrial and freshwater environments for radiological
81 assessments' (IAEA, 2009). These documents summarized a new soil K_d data compilation
82 that included approximately 2900 records for 67 elements and were a major update of the
83 previous K_d compilation (IAEA, 1994).

84 One of the main outcomes resulting from the analyses of this compilation was the
85 proposal of K_d best estimate values (as a geometric mean value) and their related variability
86 (expressed as a geometric standard deviation value, and with the minimum-maximum K_d
87 values range) (Gil-García et al., 2009a; Gil-García et al., 2009b; Vandenhove et al., 2009).
88 Partial datasets were constructed based mainly on soil groups according to the organic matter
89 (OM), and clay and sand (textural) contents of the mineral soil samples, the so-called
90 OM+Texture criterion. This approach was uniformly applied to all RNs with sufficient data to
91 permit such analysis. But even after following this approach, it was shown that the K_d data
92 could still vary more than 4 orders of magnitude within one OM+Texture soil group, thus
93 compromising the usefulness and reliability of the derived best-estimate values.

94 The Modelling and Data for Radiological Impact Assessments (MODARIA)
95 Programme was auspiced by IAEA during the period 2012 and 2015, which was followed by
96 the MODARIA II Programme (Development, Testing and Harmonization of Models and Data
97 for Radiological Impact Assessment; 2016-2019). Working groups were established whose
98 main goal was to analyse radiological data aiming at, among others, identifying the data gaps
99 of those parameters relevant for the radiological assessments; filling the priority data gaps by

100 updating previous parameter data compilations with recently available data and exploring the
101 viability of applying approaches based on the extrapolation of the current existing data to
102 foresee other scenarios lacking of data, *i.e.*, analogue approach; and developing strategies for
103 handling of variability of parameter values to provide end-users with less uncertain data for
104 radiological assessment purposes. Specifically, an aim of the working groups was to update
105 the available soil RN K_d dataset, as well as to develop a strategy to reduce and describe K_d
106 variability based on probabilistic models, including the construction of distribution functions
107 to statistically describe the K_d values of a target RN.

108 This is the first in a series of three papers, in which we describe and illustrate the
109 approach followed to derive best-estimate K_d values and K_d statistical distributions from an
110 updated and critically reviewed compilations of RN K_d values (Ramírez-Guinart et al. 2020a;
111 Ramírez-Guinart et al. 2020b). In this first paper the approach to reducing the distribution of
112 K_d values is described and illustrated for uranium K_d values. Parts two and three in this series
113 of papers show the application of the approach to radiocaesium and americium K_d values,
114 respectively. In all three papers, the most suitable criteria for reducing uncertainty, such as
115 soil characteristics (*e.g.*, pH, texture, organic matter content, etc.) and factors related to the
116 experimental approach applied (*e.g.*, sorption *vs.* desorption test, or effect of long-term
117 interaction), are evaluated; the cumulative distribution functions of K_d values for the
118 optimized groupings are proposed; and the viability of using K_d data gathered from geological
119 materials other than soils (material analogue approach) and/or for elements chemically similar
120 to the target element (chemical analogue approach) to enhance datasets containing insufficient
121 entries of the target element are assessed.

122

123

124 **2. Data collection and treatment**

125 *2.1. Soil RN K_d compilation update: revision of data acceptance criteria*

126 The former TRS-472 soil K_d data compilation was critically reviewed and updated, by
127 examining more than 100 new documents (reviewed papers and grey literature). The K_d
128 values available, along with ancillary information regarding the method used and soil
129 characteristics, such as soil pH, organic matter content, clay and silt contents in the mineral
130 fraction and cationic exchange capacity, were incorporated into the K_d compilation.

131 K_d values not directly quantified as the ratio between concentrations of the target
132 element measured in a liquid and a solid phase were rejected. Consequently, the current
133 compilation does not include data: 1) indirectly derived from parametric equations, 2)

134 indirectly deduced from mass-transport experiments, such as column tests or diffusion
135 experiments, or 3) pooled or averaged K_d values from former K_d data compilations.
136 Furthermore, K_d data originated from the same element-sample combination by applying a set
137 of tests at varying operational variables related to the experimental approach, but not
138 considered as a relevant factor for grouping K_d values (*e.g.*, contact time or solid-to-liquid
139 ratio in batch experiments) were pooled to become a single entry, calculated as a geometric
140 mean (GM). Instead, they were entered into the data base as individual entries if the variable
141 tested could be considered as a relevant factor (*e.g.*, experiments at varying pH). K_d data were
142 only accepted if they were obtained under experimental conditions representative of typically
143 environmental conditions. For example, K_d measurements measured under extreme chemical
144 conditions ($< \text{pH } 2$ or $> \text{pH } 12$) were not included. K_d data for stable isotopes were accepted
145 so long as they were obtained using isotope concentrations within the linear sorption range. In
146 agreement with the previous compilation (IAEA, 2009), K_d data from pure mineral phases,
147 such as clay minerals or metal (hydro)oxides, were not accepted. The K_d compilation also
148 included data from subsoils, surface sediments (formed by deposition of transported organic
149 matter or mineral soils by the action of wind, water, or ice, and/or by the force of gravity
150 acting on the particles), gyttja (which refer to a mud formed from organic and mineral matter,
151 which can be found at the bottom or near the shore of certain lakes) and till materials (which
152 are unsorted and non-stratified materials deposited directly by glacial ice, which consist of a
153 mixture of clay, silt, sand, gravel, stones, and boulders in any proportion).

154

155 *2.2. Structure of the updated soil RN K_d compilation: creation of partial datasets*

156 The current soil RN K_d compilation is a spreadsheet-type document in which K_d and
157 ancillary data are organized based on elements in independent sheets. It contains more than
158 5000 entries of soil K_d for 83 elements, and additional more than 2000 entries of K_d data for
159 75 elements gathered from a selection of other solid materials. Besides fields related to the
160 sources of information, radioisotopes, soil characteristics and ancillary information, new
161 fields related to the experimental approach and type of material were added. The category of
162 ‘type of material’ is used to distinguish between K_d data for soils (the unconsolidated
163 geological material comprising the terrestrial root zone) versus those from other types of
164 geological materials, such as sediment, subsoils, till and gyttja. Various categories were
165 created to classify the experimental approaches (see Table 1: short or long-term experiments;
166 in situ, batch sorption or batch desorption tests) that permit selecting K_d values for specific
167 transport scenarios. Either for the overall dataset, or from partial datasets based on the

168 experimental approach, grouping criteria based on soil factors were used to create further
169 partial datasets from which were derived K_d best estimate values and related distribution
170 function with a lower variability obtained.

171 A strategy was then developed and applied to create partial datasets with less
172 variability, based on grouping the K_d data of a given element according to optimized criteria
173 that consider factors related to the soil characteristics and the experimental approach applied,
174 relevant for the RN-soil interaction. The aim was to identify the soil properties that reduced
175 RN K_d variability, especially those routinely analysed (and, thus, more likely to have
176 available information); to establish a series of criteria to properly create K_d partial datasets;
177 and to construct cumulative distribution functions (CDFs) or, at least, to derive best-estimate
178 values for each group.

179 The OM content was the first soil property to be tested (the OM criterion), and the
180 effect of the soil texture for mineral soils was also tested when relevant (the OM+Texture
181 criterion). Thus, four soil groups were created based on the texture (Sand, Loam, and Clay
182 soils) and organic matter content (Organic soils). Initially, a soil was included in the Organic
183 group if its OM content was $>20\%$. For the mineral soils, three groups were created according
184 to the following criteria (% refers to mineral matter): Sand group: sand fraction $\geq 65\%$; clay
185 fraction $< 18\%$; Clay group: clay fraction $> 35\%$; and Loam group (IAEA, 2010). Additional
186 soil factors were also checked for specific radionuclides. For instance, the pH and hierarchical
187 application of various soil factors, such as pH and OM, were tested as described later in
188 Section 3. Finally, statistical tests (Fisher's least significant differences (FLSD) test for
189 multiple samples; 95% confidence level; StatGraphics 18) were performed to check whether
190 the geometric mean K_d values for the partial datasets were significantly ($p \leq 0.05$) different.

191

192 *2.3. Analysis of the influence of the experimental approach on RN K_d data variability*

193 The influence of the experimental approach was simultaneously evaluated along with
194 relevant soil factors. Before applying the grouping criteria based on the experimental
195 approach factor, a data treatment based on group mean centering (GMC) was carried out to
196 minimize the effect of soil factors identified as relevant to the interaction of the target
197 element. Figure 1 illustrates this approach for the pH+OM criterion as the key soil-factor for
198 the GMC treatment for U K_d values. Other soil factors may be applicable to other
199 radionuclides. The GMC consisted in log-transforming the overall dataset of the target
200 element, grouping the K_d data according to the soil criteria previously established based on a
201 key soil factor, calculating the arithmetic mean (AM) of log K_d values of each soil-type group

202 created and correcting each single $\log K_d$ value within a given group by subtracting the AM
203 $\log K_d$ value of the respective soil-type group. Secondly, the GMC-corrected $\log K_d$ datasets
204 were splitted in subsets according to the type of the experimental approach, that is, firstly
205 long- versus short-term experiments, and then a further splitting was carried out based on in
206 situ, sorption and/or desorption experiments. No in situ data were available in the current
207 datasets and, thus, it was only necessary to split the short-term partial datasets into sorption
208 and desorption categories. Finally, statistical tests (Fisher's Least Significant Differences
209 (FLSD) test for multiple samples; 95% confidence level; StatGraphics 18) were performed to
210 check whether the K_d geometric means for each partial datasets were significantly different.

211

212 *2.4. Construction of Cumulative Distribution Functions (CDF) to describe K_d variability*

213 A suitable method to describe the population and variability of K_d values for a certain RN-
214 material combination is the construction of Cumulative Distribution Functions (CDF). In
215 short, CDFs are equations describing the different values of a real-valued variable, in this case
216 K_d , and their related accumulated frequency, which means that the probability that K_d takes a
217 value less than or equal to a certain value can be explained in a continuous form with a
218 function. CDFs are built with the statistical parameters (*e.g.*, arithmetical mean, geometric
219 mean, mode, variance, etc.) of the underlying frequency distribution (*e.g.*, normal, lognormal,
220 exponential, etc.) (Ciffroy et al., 2009). Thus, in order to construct reliable CDFs it is
221 necessary to unequivocally ascertain the statistical distribution describing the data population,
222 as well as to properly derive the corresponding statistical parameters.

223 Since the K_d parameter is a ratio of concentrations, K_d data are expected to follow a
224 lognormal distribution (Sheppard et al., 2011). If a K_d dataset is lognormally distributed, then
225 it inherently implies that the log-transformed K_d values of this dataset ($\log K_d$) follows a
226 normal distribution. The statistical parameters describing a symmetrical $\log K_d$ distribution
227 are: the location parameter (μ), which can be considered as the most probable $\log K_d$ value
228 since it corresponds to the 50th percentile of the $\log K_d$ distribution, and the scale parameter
229 (σ), which gives an estimation of the dispersion among $\log K_d$ values. Both statistical
230 parameters can be determined either by calculating the arithmetic mean (AM) and standard
231 deviation (SD), respectively, of the experimental $\log K_d$ values comprising a given dataset or
232 by fitting the experimental cumulative distribution of the $\log K_d$ dataset to the theoretical CDF
233 equation of the normal distribution. Figure S1 in the Supplementary Material illustrates the
234 graphical representation of the CDF of an ideal lognormal dataset that contains K_d values
235 within the 1 to 10^6 L kg⁻¹ range. CDFs also informs of all the potential values and their

236 probability of occurrence (Ciffroy et al., 2009). Thus, confidence intervals of K_d values can
 237 also be established from a CDF constructed with a K_d dataset by calculating the
 238 corresponding percentile ranges (*e.g.*, the 90% and 95% confidence intervals correspond to
 239 the 5th - 95th and 2.5th - 97.5th percentile ranges, respectively).

240 For the construction of CDFs (see Figure S2 of the Supplementary Material), K_d data
 241 were log-transformed and the presence of possible outlier values in the datasets was examined
 242 by performing an exploratory analysis based on box-and-whisker plots. A threshold of three
 243 times the interquartile range was established to identify if a log K_d values was an outlier. The
 244 log K_d data within every dataset were sorted by increasing value and an empirical frequency
 245 ($f_{\text{exp},i}$) equal to $1/N$ (where N is the total number of K_d entries in the respective dataset) was
 246 assigned to each entry. Experimental cumulative frequency distribution were constructed by
 247 assigning to each sorted log K_d value their corresponding cumulative frequency ($F_{\text{exp},i}$), *i.e.*,
 248 the sum of the preceding frequencies ($F(K_{d,j}) = \sum_{i=0}^j f(K_{d,i})$). Following this, the
 249 Kolmogorov-Smirnov test was applied to test if the experimental cumulative distribution
 250 function did not statistically differ from the theoretical cumulative frequency distribution
 251 constructed by assuming a lognormal distribution. As expected, it was found that all the K_d
 252 datasets analysed followed a lognormal distribution. Consequently, the experimental
 253 cumulative frequency distributions constructed with the log K_d data were fitted to the
 254 theoretical normal CDF equation (Eq. 1) and the location and scale parameters (μ and σ ,
 255 respectively) were derived to construct CDFs.

256

$$257 \quad P(\log K_{d,i} \leq \log K_{d,j}) = \sum_{\log K_{d,i} \leq \log K_{d,j}} p(\log K_{d,i}) = \frac{1}{2} + \frac{1}{2} \operatorname{erf}\left(\frac{\log(K_{d,i}) - \mu}{\sigma\sqrt{2}}\right); K_{d,i} > 0. \quad [1]$$

258

259 where P is the cumulative probability, erf is the error function, and subscripts i and j represent
 260 two different K_d values in the ranked grouping.

261

262 Since the statistical parameters determined are in log-scale, the derived best-estimate value
 263 and confidence range are also in log-scale. Thus, the corresponding antilog parameters were
 264 calculated, that is, the geometric mean (GM) and geometric standard deviation (GSD), as
 265 shown in Eq. (2) and Eq. (3):

$$266 \quad \text{GM}(K_d) = \left(\prod_{i=1}^N K_{d,i}\right)^{\frac{1}{N}} = 10^{\left(\frac{1}{N} \sum_{i=1}^N \log(K_{d,i})\right)} = 10^\mu = \operatorname{antilog}(\mu) \quad [2]$$

$$267 \quad \text{GSD}(K_d) = 10^{\sqrt{\frac{\sum_{i=1}^N \left(\log \frac{K_{d_i}}{\text{GM}}\right)^2}{n}}} = 10^\sigma = \text{antilog}(\sigma) \quad [3]$$

268

269 To properly derive a reliable CDF from a given K_d dataset it is necessary that it contains a
 270 minimum number of entries (around $N > 10$). Exceptionally, from those datasets containing a
 271 lower number of entries, CDFs were constructed as far as the datasets presented clear
 272 experimental cumulative distributions and a good fitting of data could be done. For the rest of
 273 cases only GM values were calculated directly from the dataset.

274

275 **3. Example of the application of the general approach for the data analyses using** 276 **uranium K_d values**

277 *3.1. Soil factors governing U sorption: derived soil criteria to group U K_d data*

278 Uranium sorption in soils is known to be very complex and affected by several soil properties
 279 and phases, mainly pH, soil texture, specific surface area (SSA), cation exchange capacity
 280 (CEC), dissolved carbonate, amorphous iron oxides ($\text{Fe}_{\text{amorph}}$) and OM matter contents (EPA,
 281 1999b; Payne et al., 2011). Uranium oxidation state or the redox status of the experimental
 282 systems are also extremely important factors influencing U K_d values. U(IV) binds
 283 appreciable more strongly and has a much lower solubility than U(VI) (Langmuir, 1978;
 284 Vandenhove et al., 2010), which is expected to be the dominant U species in most topsoils. At
 285 pH below 5, U(VI) is present as the uncomplexed uranyl ion, UO_2^{2+} . At a higher pH, the
 286 uranyl ion hydrolyses, forming aqueous hydroxide complexes, which dominate U(VI)
 287 speciation in the absence of dissolved inorganic ligands (*e.g.*, carbonate, sulphate or
 288 phosphate). At the pH range of 5–10, highly soluble carbonate complexes dominate the U
 289 speciation (Vandenhove et al., 2010; Li et al. 2014). Few studies included in the U K_d dataset
 290 provided information about the specific U species in their system and thus this information
 291 could not be incorporated as a significant field of the dataset or be used for data treatment.
 292 In general, the sorption of U by soils is low at pH values less than 3, increases rapidly with
 293 increasing pH from 3 to 5, reaches a maximum in the pH range from 5 to 7, and then
 294 decreases with increasing pH values greater than 7 (EPA, 1999b). Thus, U sorption in soils
 295 frequently shows an inverted-U shaped trend in relation to the pH. The increase in sorption
 296 between pH 3 and 5 has been attributed to increased number of available sorption sites at clay
 297 minerals, while the decrease sorption above pH 7 has been attributed to the dominance of
 298 U(VI)-carbonate complexes that have weak affinities for mineral surfaces (EPA, 1999b).

299 Organic matter and clay minerals provide exchange sites that are expected to increase
300 sorption of UO_2^{2+} and other positively-charged U species (Kaplan and Serkiz 2001; Li et al.
301 2014; Li et al. 2015). The influence of organic matter on U interaction is twofold: an
302 increased sorption through exchange mechanisms on soil-bound OM and a decreased sorption
303 due to formation of soluble organic complexes, for those samples having large amounts of
304 dissolved organic matter content and colloids. U(VI) was found to be strongly retained by
305 organic aggregates and organic coatings on quartz minerals (Crançon and van der Lee, 2003),
306 whereas a large fraction of U(VI) was also found to be associated to humic colloids in soil,
307 thus forming a potential mobile uranium phase. Other studies also highlight the importance of
308 iron oxides/hydroxides for the sorption of U (Hsi and Langmuir, 1985; Waite et al., 1994;
309 Duff and Amrhein, 1996; Payne et al., 1996; Kaplan et al. 2016). The positively charged U-
310 species are sorbed to the negatively charged surfaces of the sesquioxides or U-species become
311 structurally incorporated in the iron-oxides (coatings) over the many dissolution–precipitation
312 cycles of these amorphous or poorly crystalline iron oxides (Sowder et al., 2003). The soil
313 specific surface area (SSA; units of $\text{m}^2 \text{kg}^{-1}$) is also known to play a significant role in
314 uranium sorption, as shown for pure mineral phases (Payne et al., 2011). Soils containing
315 large fractions of amorphous or clay minerals are expected to have very large specific surface
316 area values. Unfortunately, there were an insufficient number of U K_d experiments in the
317 literature that included specific surface area soil measurements, consequently it was not
318 possible to assess soil surface area as an independent variable for predicting U K_d values.

319 Due to the varying soil properties affecting U sorption, it is difficult to use
320 geochemical modelling or parametric equations to predict U K_d based on soil characteristics,
321 although there have been recent advances to notice. The use of the smart- K_d concept offers
322 new possibilities for the modelling of K_d for elements with complex speciation system as U,
323 as the coupling of a surface complexation model with a geochemical speciation code permits
324 to calculate more realistic distribution coefficients as a function of varying environmental
325 conditions (Stochmann et al., 2017). Using regression statistics, Echevarria et al. (2001)
326 explored the effect of soil characteristics on U sorption for a reduced soil dataset and deduced
327 a linear relationship between soil U K_d and pH that evidenced that U K_d values decreased
328 when increasing pH in the 5.5–8.8 pH range. A similar pattern was also observed by
329 Vandenhove et al. (2007) for a controlled dataset comprising soils with $\text{pH} \geq 6$, which was
330 explained by the increased amount of soluble uranyl–carbonate complexes at increasing basic
331 pH. However, Sheppard et al. (2006) found that, when considering heterogeneous dataset
332 composed by soils with pH ranging from 5.5 to 8.8 and data from varying sources, only

333 relative low percentage of U K_d variance could be explained by the U K_d vs. pH correlations
334 obtained, indicating that the U K_d cannot be univariantly predicted from pH variation.
335 Sheppard (2011) recently suggested updated K_d vs. pH and clay correlations, based on a
336 dataset enriched with a significant contribution of field data with indigenous uranium.

337 The use of soil carbonate content, or more specifically the CO_3^{2-} and HCO_3^-
338 concentration in soil solution, and the iron hydro(oxides) content or soil specific surface area
339 to group U K_d values, was not considered as this information usually is not available in the
340 current compilation. Instead, U K_d data was initially grouped according to the OM criterion to
341 distinguish between mineral and organic soils, as this approach indirectly includes the role of
342 not only organic matter but also specific surface area. To complete the examination of the
343 effect of specific surface area, the mineral dataset was splitted when possible into the different
344 textural groups. As pH strongly affects U species present in the soil solution, the U K_d overall
345 dataset was also split into three pH groups ($\text{pH} < 5$; $5 \leq \text{pH} < 7$; and $7 \leq \text{pH} < 9$) defined
346 according to the U speciation (Vandenhove et al., 2009), which defines the pH criterion.
347 Finally, it was evaluated for the first time the hierarchical application of soil factors to group
348 U K_d data (pH, pH+OM; pH+OM+Texture). Thus, the U K_d groups created when the U
349 overall dataset was firstly split according to the pH criterion were further split according to
350 the OM content to create Mineral and Organic groups (pH+OM criterion). In a further step, U
351 K_d data in the pH-Mineral groups were also split according to the soil texture into the three
352 textural groups (pH+OM+Texture criterion).

353

354 *3.2. Influence of experimental approach on U K_d data*

355 The overall U K_d dataset contained 196 entries with U K_d values varying more than 4 orders
356 of magnitude. The overall GM value was 320 L kg^{-1} (see Figure 2), in general agreement with
357 previous reported values (Sheppard et al., 2006; Vandenhove et al., 2009). However, the GM
358 or CDF that could be derived from the overall dataset are affected by a more than 4-orders of
359 magnitude uncertainty (the 5th-95th percentile range was 3.5×10^0 - $9.9 \times 10^3 \text{ L kg}^{-1}$) and they
360 may be not suitable for risk assessment in specific scenarios.

361 The overall U dataset contained entries of short-term sorption (ST-S), short-term
362 desorption (ST-D) and long-term desorption (LT-D) experimental approaches, as defined in
363 Table 1. The GMC data treatment to examine the effect of the experimental approach on U K_d
364 variability considered the combination of soil factors most relevant to U sorption, that is, pH
365 and OM. The FLSD statistical analyses performed are summarised in Table S1 of the
366 Supplementary Material. When splitting the datasets according to the partial pH+OM groups,

367 no effect of the experimental approach was observed for $U K_d$ for data obtained neither at pH
368 < 5 nor at $pH \geq 7$, and only a few non-systematic discrepancies were noticed for the $5 \leq pH <$
369 7 dataset. Therefore, as the possible effect of the experimental methodology was not
370 unequivocally proven by the statistical analyses of the partial datasets, $U K_d$ data were not
371 segregated based on experimental approach in the subsequent analyses.

372

373 *3.3. $U K_d$ best estimates and CDFs based on the OM and OM+Texture criteria*

374 The current U dataset when refined for applying the OM criterion contained 153 entries
375 varying in the same range of $U K_d$ values as the overall dataset. Figure 2 displays the data
376 obtained when applying the OM criterion as well as the graphical representation of the CDFs
377 constructed from the overall and partial datasets.

378 The $U K_d$ data in the Mineral and Organic partial datasets were significantly different
379 (Figure 2). The GM of the Organic group was around one order of magnitude greater than that
380 of the Mineral group, which confirmed the role observed in previous studies regarding the
381 enhancement of the uranium sorption due to its interaction with the soil organic matter
382 (Crançon and van der Lee, 2003). The application of the OM criterion allowed proposing
383 CDFs for the Mineral and Organic groups, which comprised K_d values varying within a
384 narrower range than in the case of the CDF constructed from the overall dataset, especially for
385 the Organic soils group. Despite this improvement, the usefulness of these CDFs for
386 performing radiological assessments may still be limited since they are constructed from
387 datasets with large variability.

388 The Mineral soils were splitted according to the soil texture and no significant
389 differences were observed in $U K_d$ data among textural groups (Clay: $GM=96 \text{ L kg}^{-1}$, $N=8$;
390 Loam: $GM=258 \text{ L kg}^{-1}$, $N=62$; and Sand= 204 L kg^{-1} , $N=28$), which did not follow a sequence
391 consistent with expected effects based on specific surface area. Thus, the OM+Texture
392 criterion to group soils did not add further relevant information than the simpler OM criterion.
393 Such results indicate that soil texture alone is not a soil factor relevant enough to control the
394 U -soil interaction and, thus, it is unnecessary to distinguish between textural soil-types for
395 mineral soils without further factors being preliminarily considered.

396 Since it was corroborated that soil OM content has a strong influence on the U
397 sorption behaviour, an exercise to optimise the threshold of OM content to consider a given
398 soil as “organic” was done. The aim of this exercise was to explore the possibility of
399 obtaining partial datasets with less variability, allowing a better distinction of those soils in
400 which the OM fraction really controls the U -soil interaction and, in turn, to succeed in

401 distinguishing $U K_d$ data of mineral soils among textural groups. The possibility was explored
402 to decrease the initial OM threshold from 20% down to 5%, by examining the new partial
403 datasets based on grouping values according to 5% and 20% OM thresholds. Results,
404 displayed in Table S2 of the Supplementary Material, showed that by lowering the threshold
405 to 5% OM there was no improvement neither in terms of decreasing the $U K_d$ variability nor
406 deriving statistically different GMs among the new mineral and organic datasets. Therefore,
407 concerning the interaction of U in soils, the initial 20% OM threshold was maintained to
408 consider whether a soil is grouped as organic or as mineral.

409

410 *3.4. $U K_d$ best estimates and CDFs based on soil factors related to U sorption mechanisms.*

411 *3.4.1. The pH criterion*

412 $U K_d$ values were initially segregated into three pH categories ($\text{pH} < 5$; $5 \leq \text{pH} < 7$; and $\text{pH} \geq$
413 7) based on U speciation. Figure 3 presents the $U K_d$ data and CDF derived by applying the
414 pH criterion, including the CDF of the overall dataset. The parameters derived from the pH
415 partial datasets were significantly different among them and contained $U K_d$ values varying
416 less than in the overall dataset, as the 5th-95th interval of $U K_d$ values decreased down to less
417 than three orders of magnitude. The derived $U K_d$ best estimates and related confidence
418 ranges indicated a significant increase in $U K_d$ values when increasing pH, reaching a
419 maximum within the 5-7 pH range, whereas $U K_d$ values decreased at higher pH values. This
420 pH-dependent U sorption agreed with previous reports (Dalvi et al., 2014; Payne et al., 2011;
421 Vandenhove et al, 2009). At low pH values ($\text{pH} < 5$) the U sorption in soils is decreased due
422 to the competition of the uranyl cation with protonated sites whereas at $\text{pH} > 7$ the decrease in
423 U sorption is caused by the formation of stable, weakly sorbing uranyl carbonate complexes.
424 The 5th-95th percentile CDF region of the $5 \leq \text{pH} < 7$ and $\text{pH} \geq 7$ partial datasets partially
425 overlapped. This fact, in conjunction with the large $U K_d$ variability still existing within the
426 pH groups from which the CDF were constructed, suggested that it was still necessary to seek
427 a more meaningful $U K_d$ grouping by means of taking into a simultaneous consideration of
428 several soil factors.

429

430 *3.4.2. Hierarchical application of pH and OM soil factors*

431 The pH+OM criterion

432 Figure 4 summarizes the $U K_d$ data obtained from the datasets created based on the
433 hierarchical application of the pH and OM soil factors (the pH+OM criterion) and depicts the
434 related CDFs. The simultaneous use of pH and OM factors led to the creation of partial

435 datasets with a much lower variability than the pH partial datasets. Besides, they followed the
436 same pH dependence as the pH-based partial datasets. Thus, for mineral soils the $U K_d$ values
437 for the intermediate pH mineral group ($5 \leq \text{pH} < 7$) were statistically the highest, whereas for
438 organic soils, as the $\text{pH} \geq 7$ data set has only 2 entries, the only significant comparison
439 showed that the GM value of the intermediate group was also higher than that of the $\text{pH} < 5$
440 organic dataset. For a given pH group, the FLSD test confirmed that organic soils always had
441 greater GMs and the 5th-95th percentile ranges were shifted to greater values than those of the
442 respective mineral group. These trends denote the suitability of using two soil factors for $U K_d$
443 grouping, as both are relevant and govern uranium soil interactions. The lack of $U K_d$ values
444 for organic soils at $\text{pH} \geq 7$ prevented the construction of the related CDF. The scarcity of such
445 data is not surprising as most organic soils have acid-to-neutral pH values. Therefore, this soil
446 group has a reduced representativity of natural environmental conditions.

447

448 The pH+OM+Texture criterion

449 A final strategy to refine the $U K_d$ data of the pH-Mineral groups was tested by splitting them
450 into textural groups according to the clay and sand content of the soils, in order to check
451 whether the absence of texture effect on $U K_d$ variability observed in section 3.3 was due to
452 not consider a previous grouping of soils by pH. As can be seen in Table S3 in the
453 Supplementary Material, most of the derived textural groups had scarce data ($N < 10$), which
454 hindered a proper evaluation of the role of introducing textural information to further decrease
455 $U K_d$ variability. As an improvement from the previous analyses, the GM of the textural
456 classes now followed the sequence based on specific surface area ($\text{GM}_{\text{Clay}} > \text{GM}_{\text{Loam}} >$
457 GM_{Sand}). Thus, the possibility of using $U K_d$ data from solid environmental materials other
458 than soils to enhance the textural datasets was explored.

459 The analogy between soils and other solid environmental materials (till, subsoil and
460 gyttja) with respect to their capacity to sorb U was evaluated. These materials were mostly
461 mineral, although a few entries of organic gyttja materials were also available. For each
462 material, all $U K_d$ data available were pooled in an overall dataset and each material and
463 partial dataset were initially created according to the pH criterion. The $U K_d$ statistics derived
464 from each dataset are summarised in Table 2. $U K_d$ data for gyttja materials had higher GMs
465 or were significantly higher than for soils (as the FLSD test revealed at $\text{pH} < 5$). Instead, $U K_d$
466 data for till and subsoils were not significantly different to the soil $U K_d$ data. From this
467 analysis it can be concluded that $U K_d$ data from tills and subsoils can be considered
468 analogous to $U K_d$ values from soils. Conversely, $U K_d$ values measured in gyttja were

469 significantly different from those of soils. Thus, available till and subsoil data, but not gyttja,
470 were used to enhance the soil subsets.

471 Table 3 summarises the data derived from the datasets in which soil and analogous materials
472 U K_d values were pooled. The inclusion of subsoil and till U K_d data on the pH+OM+Texture
473 partial datasets allowed constructing CDFs with a higher number of entries, although the pH-
474 Clay groups still lacked enough data. Although the GMs and 5th-95th percentile ranges that
475 could be derived for the pH+OM+texture groups were again consistent with the U sorption
476 mechanisms (and the expected lower specific surface area values for sandy soils), no
477 statistically significant differences were observed among the textural groups at the 95% of
478 confidence level. However, low-p values, in some cases < 0.1 , suggest that it may be
479 warranted to treat clay+loam and sand as separate textural classes, as their GM values differed
480 by more than one order of magnitude. Accordingly, the proposal of U K_d data for soil groups
481 based on pH+OM criteria, and further distinguishing clay+loam from sandy soils, is the more
482 detailed and statistically-based approach for radiological assessments from the available
483 entries in the current dataset.

484

485 **4. Conclusions and recommendations**

486 An integrated data treatment approach was demonstrated to decrease and describe K_d
487 variability by creating partial datasets based on the experimental approach and relevant soil
488 factors governing RN-soil interaction. When soil properties governing radionuclide
489 interactions are identified and datasets with a sufficient number of entries are available, this
490 approach can successfully derive best-estimate K_d values and related distribution functions
491 with a lower inherent variability. K_d values with lower variability are more useful for risk
492 assessment exercise.

493 As tested here for uranium, the analyses performed to the overall U K_d dataset
494 demonstrated that a single U K_d best-estimate value should be avoided as input data for
495 radiological risk assessment models. Instead, it is recommended that modellers make use of
496 informed data, more related to the scenario to be assessed, with as much information as
497 possible of the soil system, focusing on refining the input data according to the values of key
498 soil properties that govern uranium-soil interaction. This approach would lead to chose among
499 K_d best estimates that may differ in various orders of magnitude, as was observed here for the
500 case for U K_d (*e.g.*, sandy soils at $\text{pH} < 5$ (see Table 3; $\text{GM}=20 \text{ L kg}^{-1}$) compared to organic
501 soils within the $5 \leq \text{pH} < 7$ range (see Figure 4; $\text{GM}=8000 \text{ L kg}^{-1}$)).

502 In principle, it is not required to refine U K_d data based on RN-soil contact time
503 (short-term vs. long-term). However, soil factors had a greater effect on U K_d values and on
504 their variability than aging processes due to interaction dynamics. These conclusions cannot
505 be extrapolated to other radionuclides. In fact, it is recommended to examine the effect of the
506 experimental approach on K_d variability for each radionuclide under study. In the absence of
507 sufficient redox and U speciation data accompanying the reported U K_d values in the
508 literature, it is suggested to refine U K_d data based on both the pH and the OM content of the
509 soils of the scenarios to be assessed, and for every pH range, to distinguish between
510 clay+loam and sandy soils. However, if pH information is not available, it is recommended to
511 at least distinguish mineral and organic soils, as the latter has higher U K_d values.

512 It was evidenced that despite the efforts made to update the U K_d compilation there are
513 still evident U K_d gaps in certain soil groups, such is the case of organic soils at basic pH, or
514 clay soils, although these two scenarios are uncommon in the environment. It was
515 demonstrated that there were no statistical differences between the U K_d data gathered from
516 soils and other geological materials such as tills and subsoils. Therefore, data from these
517 analogue materials can be used to enhance the number of entries of the U K_d soil datasets and
518 contribute to their continuous update.

519 **References**

- 520 Aldaba, D., Rigol, A., Vidal, M., 2010. Diffusion experiments for estimating radiocesium and
521 radiostrontium sorption in unsaturated soils from Spain: Comparison with batch
522 sorption data. *J. Hazard. Mater.* 181, 1072.
- 523 ASTM, 2003. ASTM D4646-03 - Standard Test Method for 24-h Batch-type Measurement of
524 Contaminant Sorption by Soils and Sediments. American Society for Testing and
525 Materials, USA.
- 526 ASTM, 2010. ASTM C1733–10 - Standard Test Method for Distribution Coefficients of
527 Inorganic Species by the Batch Method. American Society for Testing and Materials,
528 USA.
- 529 Ciffroy, P., Durrieu, G., Garnier, J. M., 2009. Probabilistic distribution coefficients (K_d s) in
530 freshwater for radioisotopes of Ag, Am, Ba, Be, Ce, Co, Cs, I, Mn, Pu Ra, Ru, Sb, Sr
531 and Th. Implications for uncertainty analysis of models simulating the transport of
532 radionuclides in rivers, *J. Environ. Radioactiv.* 100, 785-794.
- 533 Crançon, P., van der Lee, J., 2003. Speciation and mobility of uranium (VI) in humic- contain
534 soils. *Radiochim. Acta*, 91 (11), 673–679.
- 535 Dalvi A. A., Kumar A. V., Reddy V. R. 2014. A site specific study on the measurement of
536 sorption coefficients for radionuclides. *Int. J. Environ. Sci. Technol.* 11, 617-622.
- 537 Degryse F., Smolders, E., Parker, D. R., 2009. Partitioning of metals (Cd, Co, Cu, Ni, Pb, Zn)
538 in soils: concepts, methodologies, prediction and applications – a review. *European*
539 *Journal of Soil Science* 60: 590-612.
- 540 Duff, M. C., Amrhein, C., 1996. U(VI) sorption on goethite and soil in carbonate solutions.
541 *Soil Sci. Soc. Am. J.* 60, 1393–1400.
- 542 Echevarria, G., Sheppard, M., Morel, J. L., 2001. Effect of pH on the sorption of uranium in
543 soils. *J. Environ. Radioactiv.* 53, 257–264.
- 544 EPA, 1999a. EPA 402-R-99-004A - Understanding variation in partition coefficient, K_d ,
545 values. Volume I: The K_d model, methods of measurement, and application of chemical
546 reaction codes, U. S. Environmental Protection Agency, USA.
- 547 EPA, 1999b. EPA 402-R-99-004B - Understanding Variation in Partition Coefficient, K_d ,
548 Values. Volume II: Review of Geochemistry and Available K_d Values for Cadmium,
549 Cesium, Chromium, Lead, Plutonium, Radon, Strontium, Thorium, Tritium (3H), and
550 Uranium, U. S. Environmental Protection Agency, USA.

551 EPA, 2001. EPA 540-R-02-002 - Risk assessment guidance for superfund: volume III - Part
552 A, Process for conducting probabilistic risk assessment, U. S. Environmental Protection
553 Agency, USA.

554 EPA, 2017. SW-846 Test Method 1315: Mass Transfer Rates of Constituents in Monolithic or
555 Compacted Granular Materials Using a Semi-Dynamic Tank Leaching Procedure, 1st
556 revision. 37 pp, U. S. Environmental Protection Agency, USA.

557 Gil-García, C., Rigol, A., Rauret, G., Vidal, M., 2008. Radionuclide sorption-desorption
558 pattern in soils from Spain. *Appl. Radiat. Isot.* 66, 126–138.

559 Gil-García, C., Rigol, A., Vidal, M., 2009a. New best estimates for radionuclide solid–liquid
560 distribution coefficient in soils. Part 1: radiostrontium and radiocaesium. *J. Environ.*
561 *Radioact.* 100, 690–696.

562 Gil-García, C., Tagami, K., Uchida, S., Rigol, A., Vidal, M., 2009b. New best estimates for
563 radionuclide solid-liquid distribution coefficients in soils. Part 3: miscellany of
564 radionuclides (Cd, Co, Ni, Zn, I, Se, Sb, Pu, Am, and others). *J. Environ. Radioact.* 100,
565 704-715.

566 Hsi, C. K. D., Langmuir, D., 1985. Adsorption of uranyl onto ferric oxy-hydroxides:
567 application of the surface complexation site-binding model. *Geochim. Cosmochim.*
568 *Acta* 49, 1931–1941.

569 IAEA, 1994. TRS-364 - Handbook of Parameter Values for the Prediction of Radionuclide
570 Transfer in Temperate Environments, International Atomic Energy Agency, Austria .

571 IAEA, 2009. TECDOC-1616 - Quantification of radionuclide transfer in terrestrial and
572 freshwater environments for radiological assessments. International Atomic Energy
573 Agency, Austria.

574 IAEA, 2010. TRS-472 Handbook of Parameter Values for the Prediction of Radionuclide
575 Transfer in Terrestrial and Freshwater Environments. International Atomic Energy
576 Agency, Austria.

577 ICRU, 2001. ICRU Report 65 - Quantities, Units and Terms in radioecology. International
578 Commission on Radiation Units and Measurements, Journal of the ICRU 1.

579 Kaplan, D. I., Serkiz, S. M. 2001. Quantification of thorium and uranium sorption to
580 contaminated sediments. *J. Radioanal. Nuclear Chem.* 248, 529-535.

581 Kaplan, D. I., Kukkadapu, R., Seaman, J. C., Arey, B. W., Dohnalkova, A. C., Buettner, S.,
582 Li, D., Varga, T., Scheckel, K. G., Jaffé, P. R. 2016. Iron mineralogy and uranium-
583 binding environment in the rhizosphere of a wetland soil. *Sci. Total Environ.* 569, 53-
584 64.

585 Langmuir, D., 1978. Uranium solution–mineral equilibria at low temperature with
586 applications to sedimentary ore deposits. *Geochim. Cosmochim. Acta* 42, 547–569.

587 Li, D., Seaman, J. C., Chang, H. S., Jaffé, P., Groos, P. K. v., Jiang, D. T., Chen, N., Lin, J.,
588 Authur, Z., Pan, Y., Scheckel, K., Newville, M., Lanzirrotti, A., Kukkadapu, R. 2014.
589 Retention and chemical speciation of uranium in an oxidized wetland sediment from the
590 Savannah River Site. *J. Environ. Radioactiv.* 131, 40-46.

591 Li, D., Kaplan, D. I., Chang, H.-S., Seaman, J. C., Jaffé, P. R., Koster van Groos, P.,
592 Scheckel, K. G., Segre, C. U., Chen, N., Jiang, D.-T. 2015. Spectroscopic evidence of
593 uranium immobilization in acidic wetlands by natural organic matter and plant roots.
594 *Environ. Sci. Technol.* 49, 2823-2832.

595 OECD, 2000. Guideline 106 - Guideline for the testing of chemicals: Adsorption-desorption
596 using a batch equilibrium method. Organisation for Economic Cooperation and
597 Development, France.

598 Payne, T. E., Brendler, V., Comarmond, M. J., Nebelung, C., 2011. Assessment of surface
599 area normalisation for interpreting distribution coefficients (K_d) for uranium sorption. *J.*
600 *Environ. Radioactiv.* 102, 888-895.

601 Payne, T. E., Davis, J. A., Waite, T. D., 1996. U sorption on ferrihydrite – effects of
602 phosphate and humic acid. *Radiochim. Acta* 74, 239–243.

603 Ramírez-Guinart, O., Kaplan, D., Rigol, A., Vidal, M. 2020a. Deriving probabilistic soil
604 distribution coefficients (K_d). Part 2: Reducing caesium K_d uncertainty by accounting
605 for experimental approach and soil type. Submitted to *J. Environ. Radioactiv.*

606 Ramírez-Guinart, O., Kaplan, D., Rigol, A., Vidal, M. 2020b. Deriving probabilistic soil
607 distribution coefficients (K_d). Part 3: Reducing variability of americium K_d best
608 estimates using soil properties and chemical and geological material analogues.
609 Submitted to *J. Environ. Radioactiv.*

610 Sheppard, M. I., Thibault, D. H., 1990. Default soil solid/liquid partition coefficients, K_d s, for
611 four major soil types: a compendium. *Health Phys.* 59, 471.

612 Sheppard, S. C., 2011. Robust Prediction of K_d from Soil Properties for Environmental
613 Assessment. *Hum. Ecol. Risk Assess.* 17(1), 263-279.

614 Sheppard, S. C., Sheppard, M. I., Tait, J. C., Sanipelli, B. L., 2006. Revision and metaanalysis
615 of selected biosphere parameter values for chlorine, iodine, neptunium, radium, radon
616 and uranium. *J. Environ. Radioactiv.* 89, 115–137.

617 Simon-Cornu, M., Beaugelin-Seiller, K., Boyer, P., Calmon, P., Garcia-Sanchez, L., Murlon,
618 C., Nicoulaud, V., Sy, M., Gonze, M. A., 2015. Evaluating variability and uncertainty in
619 radiological impact assessment using SYMBIOSE. *J. Environ. Radioactiv.* 139, 91-102.

620 Sowder, A.G., Bertsch, P.M., Morris, P.J., 2003. Partitioning and availability of uranium and
621 nickel in contaminated riparian sediments. *J. Environ. Qual.* 32, 885–898.

622 Stenhouse, M. J., 1994. Technical Report NTB 93-06 - Sorption Databases for Crystalline,
623 Marl and Bentonite for Performance Assessment. NAGRA, Switzerland.

624 Stockmann, M., Schikora, J., Becker, D.-A., Flügge, J., Noseck, U., Brendler, V. 2017. Smart
625 K_d -values, their uncertainties and sensitivities - Applying a new approach for realistic
626 distribution coefficients in geochemical modeling of complex systems. *Chemosphere*
627 187, 277-285.

628 Sy, M., Gonze, M. A., Métivier, J. M., Nicoulaud-Gouin, V., Simon-Cornu, M., 2016.
629 Uncertainty analysis in post-accident risk assessment models: application to the
630 Fukushima accident. *Annals of Nuclear Energy* 93, 94-106.

631 Vandenhove, H., van Hees, M., Wouters, K., Wannijn, J., 2007. Can we predict uranium
632 bioavailability based on soil parameters? Part 1: Effect of soil parameters on soil
633 solution uranium concentration. *Environ. Pollut.* 145, 587–595.

634 Vandenhove, H., Gil-García, C., Rigol, A., Vidal, M. 2009. New best estimates for
635 radionuclide solid-liquid distribution coefficients in soils. Part 2. Naturally occurring
636 radionuclides. *J. Environ. Radioactiv.* 100, 697-703.

637 Vandenhove, H., Hurtgen, C., Payne, T.E. 2010. “Uranium”, Radionuclides in the
638 Environment (Atwood, D.A., Ed.). John Wiley & Sons.

639 Waite, T. D., Davis, J. A., Payne, T. E., Waychunas, G. A., Xu, N., 1994. U(VI) sorption to
640 ferrihydrite: application of the surface complexation model. *Geochim. Cosmochim.*
641 *Acta* 58, 5465–5478.

Table 1Description of the experimental approach categories followed for K_d quantification.

Experimental approach categories	Examples of experiments
Short-term	<p>K_d of anthropogenic elements determined from their concentration in paired water-and-soil samples collected in areas recently ($< \sim 1$ yr) contaminated with radioisotopes or with low concentrations of stable isotopes of the target element.</p> <p>In-situ K_d of indigenous elements (radioisotopes or stable isotopes) derived from determining their concentration in paired water-and-soil samples collected in non-contaminated areas. The target element concentration in the soil-porewater and in the reversible fraction of the sorbed indigenous element (<i>e.g.</i> using mild extractant reagents, such as acetic acid 0.43M) are quantified.</p>
	<p>K_d of elements derived from applying a sorption batch test based on putting in contact for short times ($< \sim 1$ yr) a clean soil (initially non-contaminated) with a solution spiked with radioisotopes or with low concentrations of stable isotopes of the target element. Soil bound radionuclide concentrations are derived by difference between aqueous radioisotope concentration before and after contact with the soil.</p>
	<p>Desorption K_d of anthropogenic elements derived from estimating the solid material concentration by applying an extraction batch test to soils recently contaminated with radioisotopes or with low concentrations of stable isotopes of the target element (<i>e.g.</i>, soil residues coming from a previous sorption test or soils sampled from recently contaminated areas). The aqueous concentration used in the K_d calculation is the concentration of the target radionuclide in the contact solution.</p> <p>K_d of indigenous elements (radioisotopes or stable isotopes) derived from estimating the solid phase concentration by applying an extraction test to contaminated solid materials when only the reversible fraction of the sorbed indigenous element is quantified (<i>e.g.</i>, using mild extractant reagents, such as ammonium acetate 1M or acetic acid 0.43M). The aqueous concentration is the concentration of the target radionuclide in the contact solution.</p>
Long-term	<p>In-situ K_d Similar to “Short-term/In-situ K_d Experimental Approach” except conducted with soils aged with target element or radionuclide for > 1 yr.</p>
	<p>Desorption K_d Similar to “Short-term/Desorption K_d Experimental Approach” except conducted with soils aged with target indigenous element or radionuclide for > 1 yr.</p>

Table 2

Descriptors of U K_d ($L\ kg^{-1}$) distributions derived from soils and other environmental materials after applying the pH criterion.

Dataset	Material	N	GM	GSD	FLSD ¹	5 th	95 th
pH < 5	Soils	53	1.5×10^2	7.8	a	3.5×10^0	1.6×10^3
	Till	8	3.5×10^2	8.8	a	2.6×10^0	3.6×10^3
	Subsoil	9	1.0×10^2	5.0	a	2.6×10^1	5.0×10^3
	Gyttja	11	3.4×10^3	3.7	b	8.0×10^2	4.4×10^4
$5 \leq \text{pH} < 7$	Soils	68	1.0×10^3	5.2	a	8.3×10^1	1.5×10^4
	Till*	5	1.5×10^3	2.6	a	n.a.	n.a.
	Subsoil	13	2.2×10^3	8.7	a	7.9×10^0	1.0×10^4
	Gyttja*	2	1.6×10^3	n.a.	-	n.a.	n.a.
pH ≥ 7	Soils	75	1.0×10^2	9.5	a	1.3×10^0	3.7×10^3
	Till	7	8.0×10^1	12	a	8.1×10^{-1}	3.7×10^2
	Subsoil	24	4.7×10^1	11	a	6.3×10^{-1}	1.7×10^3
	Gyttja*	2	6.6×10^2	n.a.	-	n.a.	n.a.

N = number of observations, GM = geometric mean, GSD = geometric standard deviation

¹ Different letters among the datasets compared indicate statistically significant differences between GMs according to the Fisher's Least Significant Differences test.

*CDF not constructed due to lack of K_d data ($N \ll 10$); n.a.: not applicable

Table 3

Descriptors of U K_d ($L\ kg^{-1}$) distributions based on the pH+OM+Texture criterion, including data gathered from soils and from solid materials analogous to soils.

Partial dataset		N	GM	GSD	FLSD ¹	FLSD ¹	5 th	95 th
pH < 5	Mineral	58	1.6×10^2	7.3	a		3.0×10^0	3.6×10^3
	Clay*	1	4.8×10^2	n.a.		-	n.a.	n.a.
	Loam	15	2.2×10^2	3.6		a	1.6×10^1	1.6×10^3
	Clay+Loam	16	2.6×10^2	3.5		a	1.6×10^1	1.6×10^3
	Sand	17	2.0×10^1	16		a	7.0×10^{-1}	6.7×10^3
$5 \leq \text{pH} < 7$	Mineral	73	1.0×10^3	5.3	b		4.6×10^1	1.0×10^4
	Loam	42	1.2×10^3	3.9		a	1.5×10^2	1.0×10^4
	Sand	15	7.2×10^2	4.6		a	8.3×10^1	6.7×10^4
pH ≥ 7	Mineral	95	8.0×10^1	9.1	c		9.4×10^{-1}	2.0×10^3
	Clay	7	2.1×10^2	7.7		a	5.0×10^0	4.7×10^2
	Loam	42	1.0×10^2	9.0		a	1.2×10^0	2.0×10^3
	Clay+Loam	49	1.0×10^2	8.7		a	1.2×10^0	2.0×10^3
	Sand	13	3.5×10^1	4.6		a	7.0×10^0	1.3×10^3

N = number of observations, GM = geometric mean, GSD = geometric standard deviation

¹ Different letters among the datasets compared indicate statistically significant differences between GMs according to the Fisher's Least Significant Differences test.

*CDF not constructed due to lack of K_d data ($N \ll 10$); n.a.: not applicable

Figure captions

Fig. 1. Illustration of the Group Mean Centering (GMC) statistical approach used to minimize the effect of soil factors identified as relevant to the interaction of the target element. In this example, the effects of the pH+OM criterion on experimental approach datasets are corrected. AM(#) is the arithmetic mean for grouping #; FLSD is the Fisher's least significant differences test.

Fig. 2. CDFs and descriptors of $U K_d$ ($L\ kg^{-1}$) distributions for Mineral and Organic soil-types (data for the Overall dataset are included for comparison). Points indicate individual dataset values whereas lines indicate the fitted distributions.

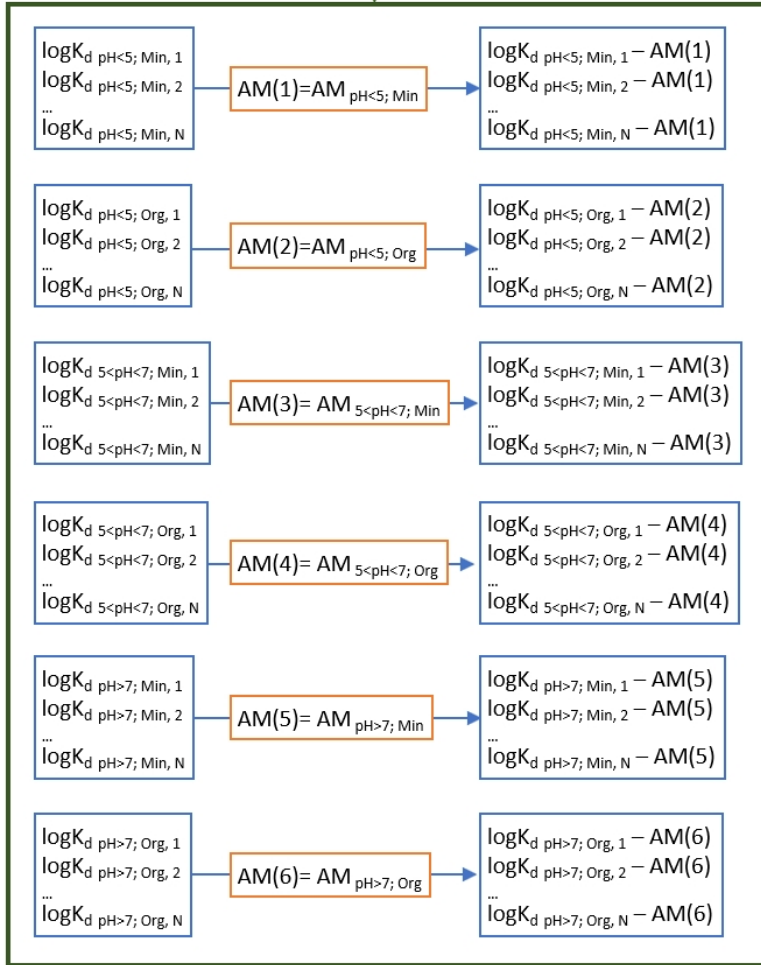
Fig. 3. CDFs and descriptors of $U K_d$ ($L\ kg^{-1}$) distributions for pH groups.

Fig. 4. CDFs and descriptors of $U K_d$ ($L\ kg^{-1}$) distributions for soil-types according to the pH + OM criterion.

K_d dataset

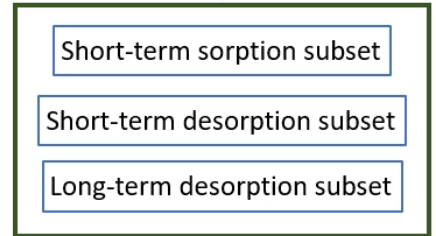
log K_d dataset

log K_d grouping according to pH+OM criterion



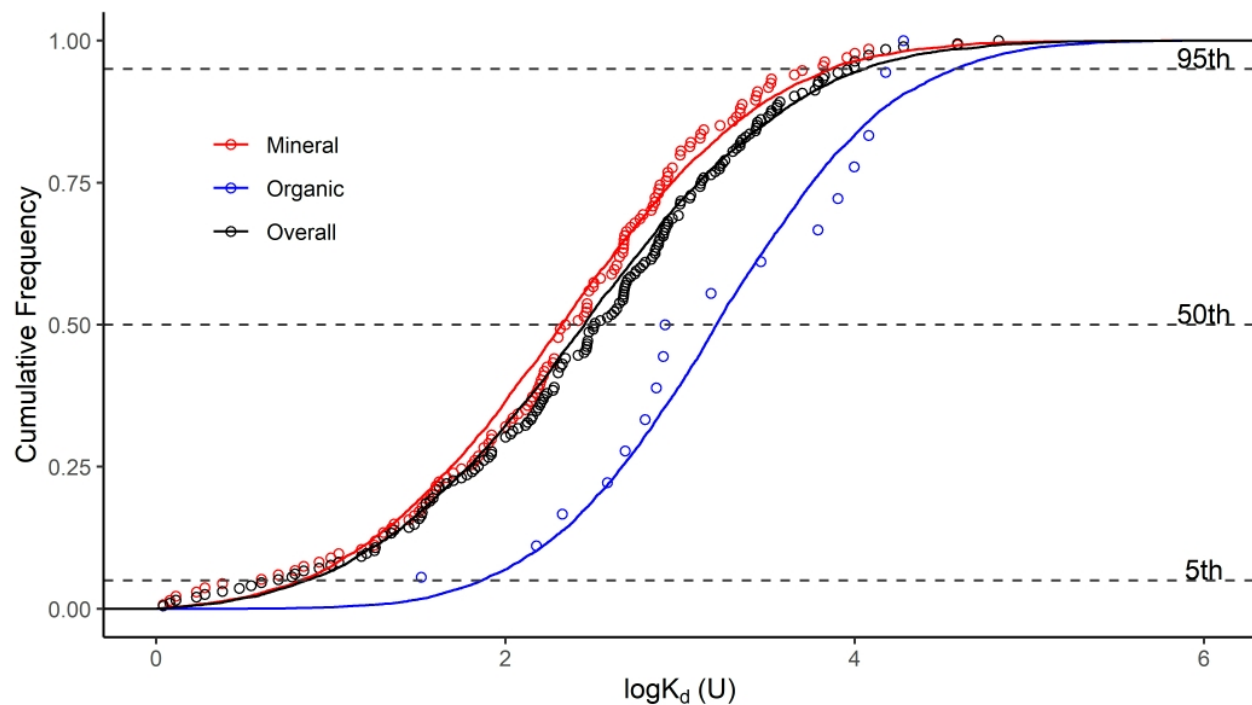
GMC log K_d dataset

GMC log K_d grouping according to the experimental approach



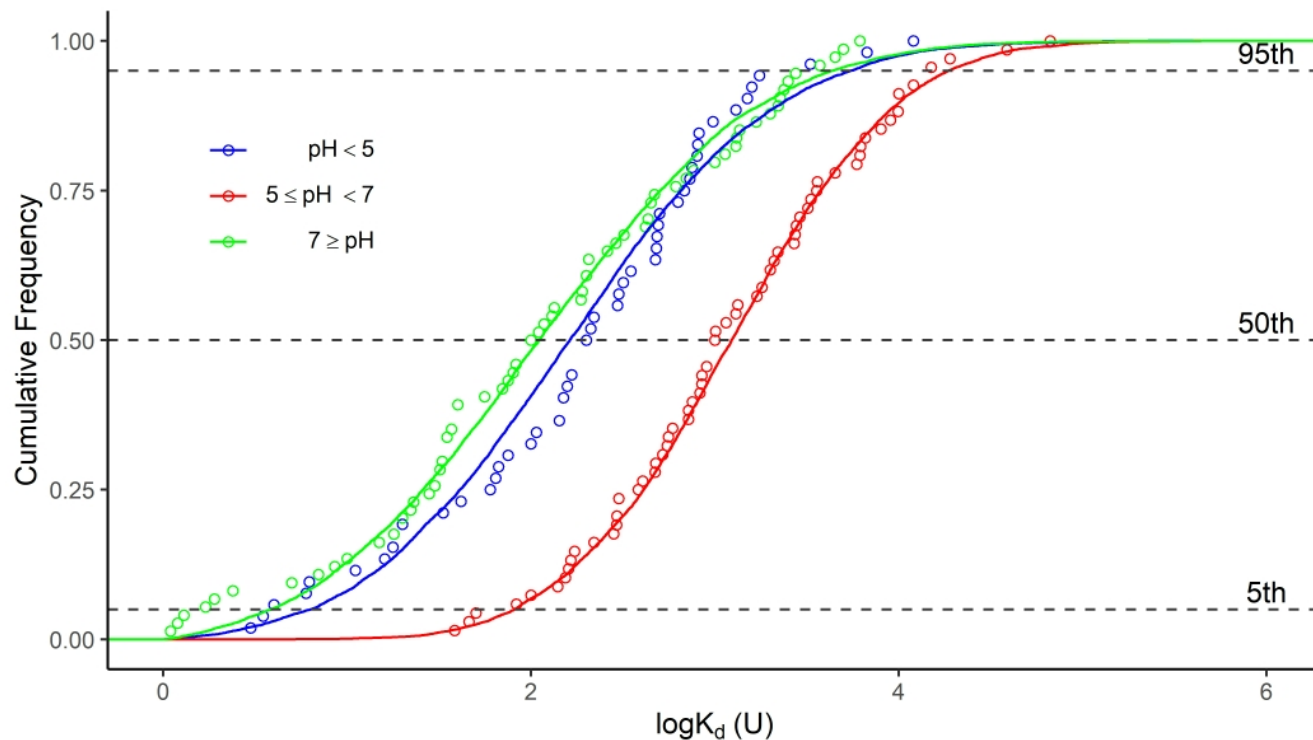
FLSD test

Statistical differences?



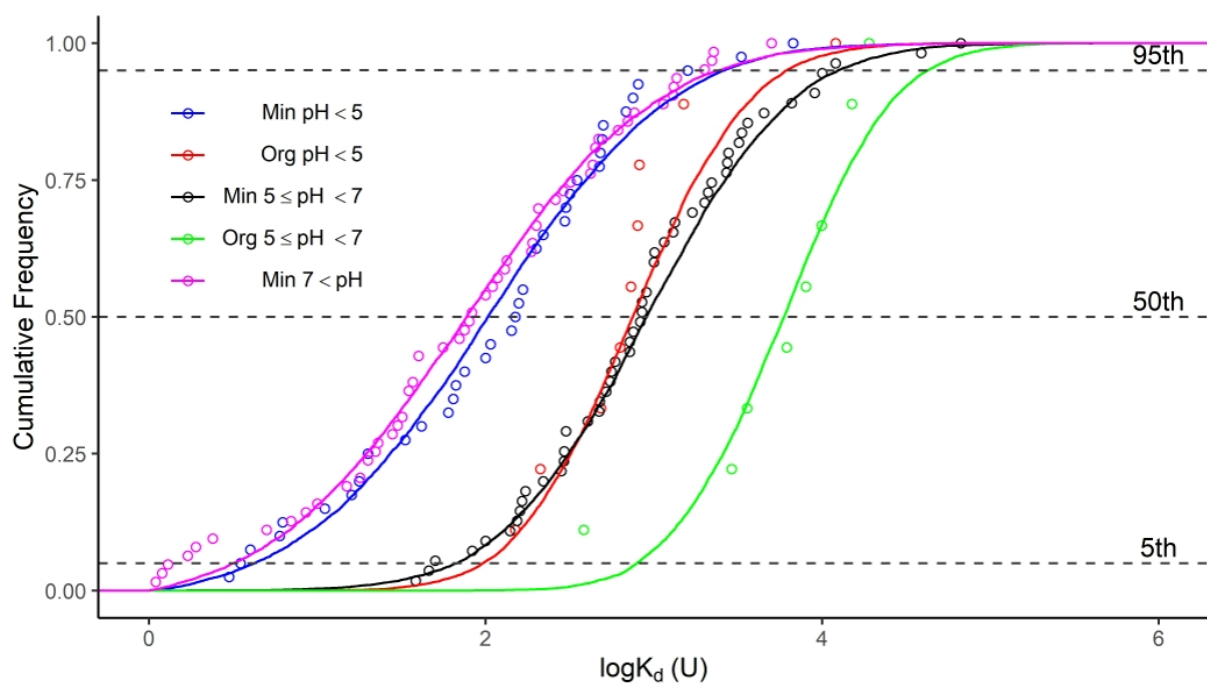
Partial dataset	N	GM	GSD	FLSD ¹	5 th	95 th
Overall	196	3.2×10^2	9.8	a	3.5×10^0	9.9×10^3
Mineral+Organic	153	3.0×10^2	9.3	a	4.0×10^0	1.0×10^4
Mineral (OM < 20%)	135	2.2×10^2	8.7	a	2.4×10^0	6.6×10^3
Organic (OM \geq 20%)	18	1.1×10^3	6.4	b	3.3×10^1	1.9×10^4

N = number of observations, GM = geometric mean, GSD = geometric standard deviation
¹ Different letters among the datasets compared indicate statistically significant differences according to the Fisher's Least Significant Differences test.



Partial dataset	N	GM	GSD	FLSD ¹	5 th	95 th
pH < 5	53	2.0×10^2	7.8	a	3.5×10^0	3.3×10^3
$5 \leq \text{pH} < 7$	68	1.0×10^3	5.2	b	8.3×10^1	1.5×10^4
pH ≥ 7	75	1.0×10^2	9.5	a	1.3×10^0	3.7×10^3

N = number of observations, GM = geometric mean, GSD = geometric standard deviation
¹ Different letters among the datasets compared indicate statistically significant differences according to the Fisher's Least Significant Differences test.



Partial dataset		N	GM	GSD	FLSD ¹	5 th	95 th
pH < 5	Mineral	41	1.5×10^2	7.4	a	3.5×10^0	1.6×10^3
	Organic	9	7.3×10^2	3.5	b	1.5×10^2	1.2×10^4
$5 \leq \text{pH} < 7$	Mineral	55	8.5×10^2	5.0	a	5.0×10^1	1.2×10^4
	Organic	9	8.0×10^3	3.4	b	3.8×10^2	1.9×10^4
pH ≥ 7	Mineral	64	8.1×10^1	8.2	n.a.	1.3×10^0	2.0×10^3
	Organic*	2	4.5×10^2	n.a.	n.a.	n.a.	n.a.

N = number of observations, GM = geometric mean, GSD = geometric standard deviation

¹Different letters among the datasets compared indicate statistically significant differences according to the Fisher's Least Significant Differences test.

*CDF not constructed due to lack of K_d data ($N \ll 10$); n.a.: not applicable

SUPPLEMENTARY MATERIAL

Deriving probabilistic soil distribution coefficients (K_d). Part 1: General approach to decreasing and describing variability and example using uranium K_d values

Table S1Effect of the experimental approach and pH and mineral grouping on U K_d values.

pH Group	Organic + Mineral Group	Experimental Approach ¹	N	FLSD ²
pH < 5	Mineral	ST-S	8	a
		ST-D	17	a
		LT-D	4	a
	Organic	ST-S	-	-
		ST-D	2	-
		LT-D	7	-
	Min+Org	ST-S	8	a
		ST-D	19	a
		LT-D	11	a
5 ≤ pH < 7	Mineral	ST-S	18	a
		ST-D	20	b
		LT-D	11	a
	Organic	ST-S	2	-
		ST-D	-	-
		LT-D	5	-
	Min+Org	ST-S	20	ab
		ST-D	20	b
		LT-D	16	a
pH ≥ 7	Mineral	ST-S	32	a
		ST-D	1	-
		LT-D	24	a
	Organic	ST-S	2	-
		ST-D	-	-
		LT-D	-	-
	Min+Org	ST-S	34	a
		ST-D	1	-
		LT-D	24	a

¹ Experimental approach: ST-S = Short-term sorption; ST-D = Short-term desorption; LT-D = Long-term desorption.

² Fisher's Least Significant Difference. Different letters among the datasets compared indicate statistically significant differences according to the Fisher's Least Significant Differences test.

Table S2Optimisation of the OM% threshold to define organic and mineral soils for U K_d

Partial data set	N	GM	GSD	FLSD ¹
Mineral (OM < 5%)	82	1.6×10^2	7.0	a
Mineral (OM < 20%)	119	2.2×10^2	7.9	a
Organic (OM \geq 5%)	52	6.8×10^2	9.0	b
Organic (OM \geq 20%)	15	1.8×10^3	7.4	b

¹ Different letter among the datasets compared indicate statistically significant differences according to the Fisher's Least Significant Differences test.

Table S3

Descriptors of U K_d ($L\ kg^{-1}$) distributions based on the pH+OM+Texture criterion for mineral soils.

Partial dataset		N	GM	GSD	FLSD ¹	5 th	95 th
pH < 5	Clay*	1	4.8×10^2	n.a.	-	n.a.	n.a.
	Loam	10	2.6×10^2	3.7	a	1.6×10^1	1.6×10^3
	Sand	14	1.4×10^1	18	a	7.0×10^1	6.7×10^3

$5 \leq \text{pH} < 7$	Loam	34	1.0×10^3	4.2	a	1.4×10^2	1.2×10^4
	Sand	13	5.6×10^2	5.0	a	8.3×10^1	6.7×10^4

pH ≥ 7	Clay	7	2.1×10^2	7.7	a	5.0×10^0	4.7×10^2
	Loam	33	7.5×10^1	10	a	1.1×10^0	2.2×10^3
	Sand	11	3.5×10^1	5.0	a	7.0×10^0	1.3×10^3

N = number of observations, GM = geometric mean, GSD = geometric standard deviation

¹ Different letter among the datasets compared indicate statistically significant differences according to the Fisher's Least Significant Differences test.

*CDF not constructed due to lack of K_d data ($N \ll 10$); n.a.: not applicable

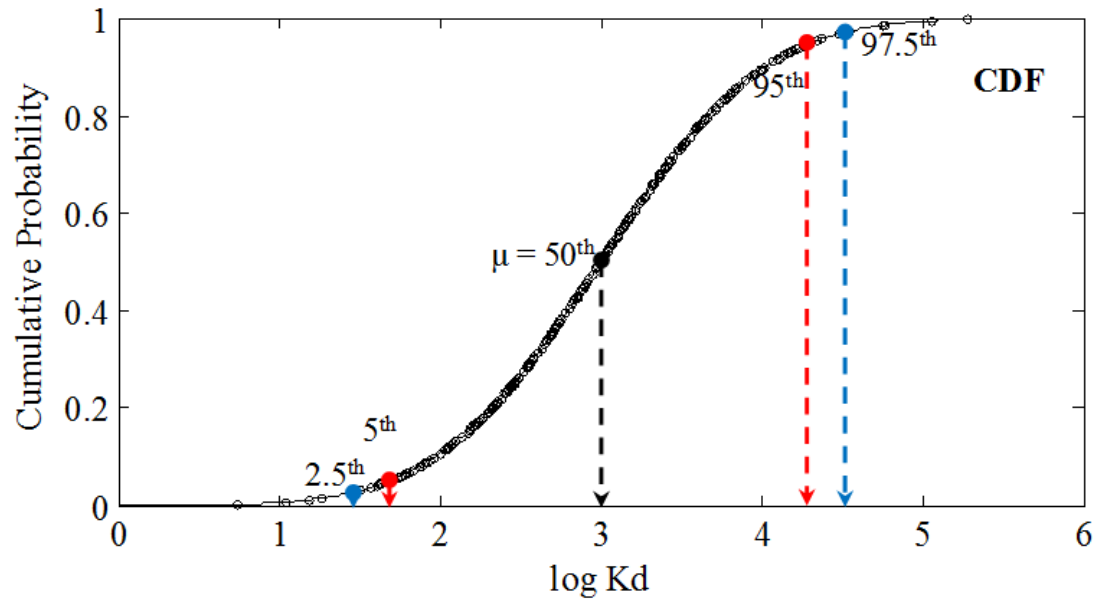


Fig. S1. Graphical representation of the CDF of an ideal lognormally distributed K_d dataset.

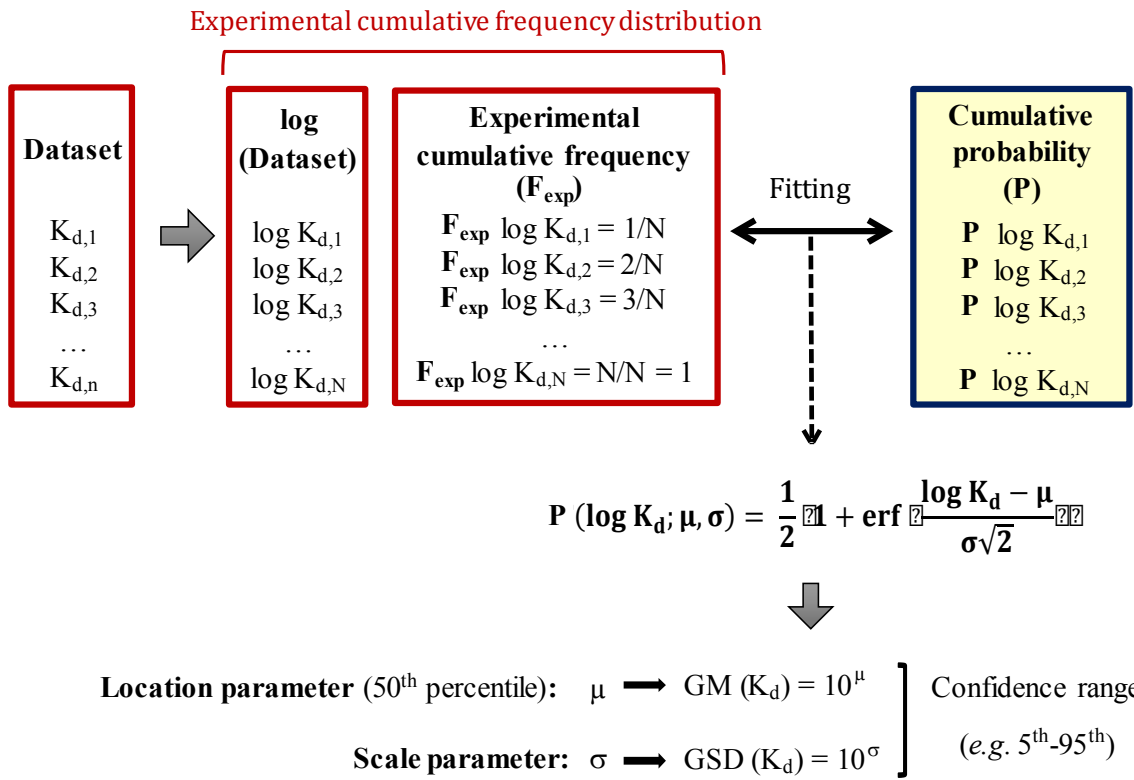


Fig. S2. Schematic process to construct CDFs and to derive best estimates values and related confidence intervals from K_d datasets.